

UC Irvine

UC Irvine Previously Published Works

Title

The Myoblast C2C12 Transfected with Mutant Valosin-Containing Protein Exhibits Delayed Stress Granule Resolution on Oxidative Stress.

Permalink

<https://escholarship.org/uc/item/4r79g5jk>

Journal

The American journal of pathology, 186(6)

ISSN

0002-9440

Authors

Rodriguez-Ortiz, Carlos J
Flores, Julio C
Valenzuela, Joanna A
et al.

Publication Date

2016-06-01

DOI

10.1016/j.ajpath.2016.02.007

Copyright Information

This work is made available under the terms of a Creative Commons Attribution License, available at <https://creativecommons.org/licenses/by/4.0/>

Peer reviewed



MUSCULOSKELETAL PATHOLOGY

The Myoblast C2C12 Transfected with Mutant Valosin-Containing Protein Exhibits Delayed Stress Granule Resolution on Oxidative Stress



Carlos J. Rodriguez-Ortiz,* Julio C. Flores,* Joanna A. Valenzuela,* Gema J. Rodriguez,* Joannee Zumkehr,* Diana N. Tran,* Virginia E. Kimonis,[†] and Masashi Kitazawa*

From the Molecular and Cell Biology,* School of Natural Sciences, University of California, Merced; and the Department of Pediatrics,[†] Division of Genetics and Genomics Medicine, University of California Irvine, Irvine, California

Accepted for publication
February 16, 2016.

Address correspondence to
Masashi Kitazawa, Ph.D.,
School of Natural Sciences,
University of California, 394
Science and Engineering, 5200
N. Lake Rd., Merced,
CA 95343. E-mail:
mkitazawa@ucmerced.edu.

Valosin-containing protein (VCP) mutations cause inclusion body myopathy with Paget disease and frontotemporal dementia. However, the mechanisms by which mutant VCP triggers degeneration remain unknown. Here, we investigated the role of VCP in cellular stress and found that the oxidative stressor arsenite and heat shock—activated stress responses evident by T-intracellular antigen-1—positive granules in C2C12 myoblasts. Granules also contained phosphorylated transactive response DNA-binding protein 43, ubiquitin, microtubule-associated protein 1A/1B light chains 3, and lysosome-associated membrane protein 2. Mutant VCP produced more T-intracellular antigen-1—positive granules than wild-type in the postarsenite exposure period. Similar results were observed for other granule components, indicating that mutant VCP delayed clearance of stress granules. Furthermore, stress granule resolution was impaired on differentiated C2C12 cells expressing mutant VCP. To address whether mutant VCP triggers dysregulation of the stress granule pathway *in vivo*, we analyzed skeletal muscle of aged VCP_{R155H}-knockin mice. We found significant increments in oxidated proteins but observed the stress granule markers RasGAP SH3-binding protein and phosphorylated eukaryotic translation initiation factor 2 α unchanged. The mixed results indicate that mutant VCP together with aging lead to higher oxidative stress in skeletal muscle but were insufficient to disrupt the stress granule pathway. Our findings support that deficiencies in recovery from stressors may result in attenuated tolerance to stress that could trigger muscle degeneration. (*Am J Pathol* 2016, 186: 1623–1634; <http://dx.doi.org/10.1016/j.ajpath.2016.02.007>)

Mutations in the valosin-containing protein (VCP) gene cause a rare hereditary disease called inclusion body myopathy associated with Paget disease of bone and frontotemporal dementia (IBMPFD).^{1,2} Some of these mutations are also attributed to cause familial amyotrophic lateral sclerosis (ALS).³ The disease penetrance, however, is different between IBMPFD and ALS or even within IBMPFD.^{4,5} Although 80% to 90% of IBMPFD patients develop inclusion body myopathy, the penetrance for frontotemporal dementia or Paget disease is significantly less, ranging from 30% to 50%, respectively.^{4,5} In the case of skeletal muscle, pathologic features include weakness and skeletal muscle atrophy. Progressive muscle wasting affects respiratory muscles and the heart, leading to respiratory and cardiac

failures, which are the main cause of death in these patients.⁵ At the cellular level, pathologic hallmarks include rimmed vacuoles positive for microtubule-associated protein 1A/1B-light chain 3 (LC3),⁶ abnormal buildup of ubiquitylated proteins, and mislocalization of transactive response DNA-binding protein 43 (TDP-43) to the cytoplasmic compartment in muscle fibers.^{7,8} Interestingly, distribution of VCP appears unaltered in affected cells.⁹

VCP is a highly conserved ATPase composed of two ATPase domains (D1 and D2), two linker domains (L1 and L2),

Funded by the NIH, National Institute of Arthritis and Musculoskeletal and Skin Diseases (NIAMS) grant R00AR054695 (M.K.).

Disclosures: None declared.

and the amino and carboxyl terminal domains.⁴ Physiologically, VCP participates in a wide variety of cellular functions, including proteasome-mediated and endoplasmic reticulum-associated protein degradation and handling of protein aggregates,^{10,11} DNA repair, and regulation of autophagy.¹² Dysregulation of these functions directly affects the survival of cells and may trigger cell death pathways.

In addition, VCP plays a key role in cellular mechanisms aimed to defend against different kinds of cellular stress. These include, but are not limited to, oxidative stress, changes in temperature, inflammation, and mechanical stress. To cope with these endogenous and exogenous kinds of stress, cells produce transient cytoplasmic aggregates denominated stress granules, composed in large part of translationally silent mRNAs and RNA binding proteins.¹³ Growing evidence strongly suggests that deficiencies in VCP function impair tolerance to cellular stress.^{14,15} Inhibition of VCP, autophagy, or lysosome produces stress granules with an altered composition, indicating that VCP and the autophagy/lysosome pathway are involved in stress granule dynamics.¹⁵ Furthermore, inactivation of VCP leads to accumulation of stress granules in yeast and mammalian cells, suggesting that VCP is required for stress granule clearance.¹⁴

Incomplete penetrance of the three different pathologic components in IBMPFD cases may be indicative that, in addition to genetic, environmental factors trigger or favor the development of discrete pathologic processes associated with mutant VCP. Although it is challenging to establish clear cause-effect relation between environmental factors and degenerative diseases, some evidence suggests an association between the two of them.^{16,17} In this regard, arsenic is one of the most toxic metalloids that exist in the soil and water. This pollutant can be found in fresh and salt water and consequently, in plants and animals in affected regions. In contaminated areas, arsenic concentration can be as high as 8.5 mg/L, almost 200 times more than the current accepted standard concentration of 0.05 mg/L.¹⁸ In a biological context, consumption of water and food with considerable amounts of arsenic can lead to a variety of diseases, including dermatosis, several different kinds of cancer, vascular diseases, and hyperkeratosis.¹⁹ Arsenic enters the cells through aquaglyceroporins because of its similar structure to glycerol.¹⁸ Inside cells, arsenic binds a variety of enzymes that possess reactive sulfur atoms and produces elevated amounts of oxidative stress. The mechanisms by means of which arsenic causes oxidative stress are not fully understood; however, it has been shown that arsenic generates imbalance of the oxido-reduction state of the cell, leading to the production of reactive oxygen species and induction of stress proteins such as the 70-kDa heat shock protein.^{19,20} Dysregulation of cellular stress management produced by mutations on the *VCP* gene, together with chronic exposure to arsenic and other stress-inducing pollutants, could facilitate the progression of the disease. Here, we present that mutant VCP significantly impaired the stress response in C2C12 cells. Cells were exposed to the oxidative stressor arsenite²¹

or heat shock, and stress granule composition, formation, and resolution were analyzed. We observed deficits in the resolution phase of the arsenite-induced stress response when mutant VCP was expressed, reflected by a delayed clearance of stress granules. However, no differences were observed between wild-type and mutant VCP on heat shock. Characterization of stress granules found that both arsenite- and heat shock-induced cellular stress produced stress granules that include TDP-43, phosphorylated TDP-43 (ser409/410), and ubiquitin. In addition, significantly lower colocalization was observed between the autophagosome- and lysosome-associated proteins, LC3 and lysosome-associated membrane protein 2 (LAMP2) and stress granules. To further address whether the presence of mutant VCP leads to dysregulation of the stress granule pathway on skeletal muscles, we quantitatively analyzed quadriceps of the VCP_{R155H}-knockin (KI) mouse model of IBMPFD. In aged VCP_{R155H}-KI mice, we observed significantly higher levels of ubiquitylated and oxidated proteins than age-matched wild-type littermates, indicative of elevated cellular and oxidative stress in the skeletal muscle of VCP_{R155H}-KI mice. However, steady-state levels of the stress granule markers RasGAP SH3-binding protein (G3BP) and phosphorylated and eukaryotic translation initiation factor 2 α (eIF2 α) remained unchanged. Immunohistochemical analysis found no differences between genotypes for G3BP, T-intracellular antigen-1 (TiA-1), and TDP-43 proteins. These *in vivo* results suggest possible compensatory mechanisms to cope with stress in chronic conditions. Yet, accumulation of modified proteins could still be detrimental and may trigger pathologic stress responses in later ages. Taken together, our results indicate that IBMPFD-relevant VCP mutations impair tolerance to stress response, leading to slower recovery of stress granule resolution after acute exogenous stress.

Materials and Methods

C2C12 Cell Culture, Differentiation, and Transfection

Cells were seeded at 70% confluence in 6-well plates or chambered cover glasses. Twenty-four hours later, cells were transfected with 1 μ g/mL human wild-type VCP(wt), VCP(R155H), or VCP(A232E) fused to dsRED (kindly provided by Dr. J. Paul Taylor, St. Jude Children's Research Hospital, Memphis, TN) with the use of turbofect according to the manufacturer's instructions (Thermo Scientific, Waltham, MA). One day later, cells were treated and processed for immunofluorescence or nuclear/cytoplasmic fractionation.

Stress-inducing treatments were 200 μ mol/L arsenite for 60 minutes and 42°C for 30 minutes. Sodium arsenite (10 mmol/L; Sigma-Aldrich, St. Louis, MO) was prepared in sterile water and diluted to 200 μ mol/L with complete Dulbecco's modified Eagle's medium before use.

To inhibit autophagy, cells were treated for 3 hours with 12 μ mol/L MHY-1485, and to inhibit lysosomal function, cells were incubated for 24 hours with 20 μ mol/L leupeptin.

For differentiation experiments, C2C12 cells were seeded at 70% confluence in 8-well plastic slides. Twenty-four hours later, cells were transfected with 1.5 $\mu\text{g}/\text{mL}$ as described above and changed to Dulbecco's modified Eagle's medium 2% horse serum to induce differentiation. Five days later, cells were treated and processed for immunofluorescence.

Tissue Preparation for Immunoblot Analysis

After deep anesthetization with sodium pentobarbital, 15- to 18-month-old mice were perfused transcatheterially with 0.1 mol/L phosphate-buffered saline (PBS), pH 7.4. Protein extracts were prepared by homogenizing quadriceps tissue in T-PER extraction buffer (150 mg/mL; Pierce, Rockford, IL), complemented with protease and phosphatase inhibitors (Sigma-Aldrich), and followed by centrifugation at $20,000 \times g$ for 15 minutes. Protein concentration was determined with the Bradford assay (Bio-Rad, Hercules, CA). For oxyblot assay (EMD Millipore, Norwood, OH), 10 μg protein were 2,4-dinitrophenyl-derivatized and detected according to the manufacturer's instructions. All animal procedures and use were performed in strict accordance with NIH's *Guide for the Care and Use of Laboratory Animals*²² and University of California Institutional Animal Care and Use Committee protocol no. AUP14-0014.

Cell Immunofluorescence

After treatment, cells were fixed in PBS + 4% paraformaldehyde (pH 7.4). After tris-buffered saline (TBS) washes, cells were incubated with TBS and Tween 20 + 3% bovine serum albumin (BSA) for 10 minutes and blocked in TBS + 1% BSA + 5% goat serum for 1 hour. Cells were incubated 18 to 72 hours with one or two of the following primary antibodies: anti-TiA-1 (dilution 1:50; Santa Cruz Biotechnology, Santa Cruz, CA; G11), TDP-43 (dilution 1:500; ProteinTech, Rosemont, IL; 12892-1-AP), phosphorylated TDP-43 S409/410 (dilution 1:500; Cosmo Bio Co, Carlsbad, CA; TIP-PTD-P01), ubiquitin (dilution 1:500; Dako, Carpinteria, CA; Z0458), VCP (dilution 1:2000; Pierce, Rockford, IL; MA3-004), LC3 I/II (dilution 1:500; Abnova, Walnut, CA; PAB12534), LAMP2 (dilution 1:500; Abcam, Cambridge, MA; ABL-93), or G3BP (dilution 1:500; ProteinTech, 13057-2-AP) in TBS + 1% BSA + 2% goat serum at 4°C. After washes, cells were incubated with the appropriate secondary Alexa Fluor-conjugated antibody (dilution 1:200; Life Technologies, Carlsbad, CA) at room temperature for 1 hour, washed, and incubated with 300 nmol/L DAPI (Invitrogen, Carlsbad, CA) for 5 minutes. Cover glasses were placed on gelatin-coated slides with Fluoromount-G (SouthernBiotech, Birmingham, AL).

Stress granules were examined under an EVOS FL (Advanced Microscopy Group, Bothell, WA) fluorescence microscope with the use of a 40 \times objective. Two variables were quantified: the number of cells positive for granules (100 cells per well; five to six wells per condition) and the

number of TiA-1⁺ granules that were also positive for a second marker (eg, TDP-43 or ubiquitin) (20 cells per well; five to six wells per condition). In the case of transfected cells, only dsRED⁺ cells were included in the analysis.

Immunohistochemistry

For skeletal muscle immunofluorescence, calf muscle was dissected and immersed in liquid nitrogen-cold 2-methylbutane and was immediately transferred to dry ice. Twenty-micron sections were obtained with a Leica cryostat (CM1860). Tissue was fixed in PBS + 4% paraformaldehyde (pH 7.4). After TBS washes, tissue was incubated with TBS and Tween 20 + 3% BSA for 30 minutes and blocked in TBS + 1% BSA + 5% goat serum for 1 hour. Tissue was incubated approximately 18 hours with one of the following primary antibodies: anti-TiA-1 (dilution 1:50; Santa Cruz Biotechnology; G11), TDP-43 (dilution 1:500; ProteinTech; 12892-1-AP), or G3BP (dilution 1:500; ProteinTech; 13057-2-AP) in TBS + 1% BSA + 2% goat serum at 4°C. After washes, tissue was incubated with the appropriate secondary Alexa Fluor-conjugated antibodies (dilution 1:200; Life Technologies) at room temperature for 2 hours, washed, and incubated with 300 nmol/L DAPI (Invitrogen) for 5 minutes. Cover glasses were placed on gelatin-coated slides with Fluoromount-G (SouthernBiotech).

Hematoxylin and eosin staining was performed on 20- μ sections fixed in 4% paraformaldehyde for 15 minutes. Sections were incubated in alum-hematoxylin solution for 5 minutes and counterstained with eosin-Phloxine B for 5 minutes, dehydrated, and cleared with CitriSolv (Fisher Scientific). Cover glasses were placed on gelatin-coated slides with Permount (Fisher Scientific, Pittsburgh, PA).

Nuclear-Cytoplasmic Fractionation

After exposure, cells were washed once with PBS and trypsinized. Cells were centrifuged at $1000 \times g$ for 4 minutes at 4°C, washed again with PBS, and resuspended in a buffer that contained 10 mmol/L HEPES, pH 7.9, 1.5 mmol/L MgCl_2 , 10 mmol/L KCl, 0.5 mmol/L dithiothreitol, 0.1% to 0.2% Triton X-100, proteases, and phosphatases inhibitors (Sigma-Aldrich). Cell membranes were disrupted with a Dounce homogenizer (20 strokes 'tight' pistil). Samples were incubated on ice for 20 minutes and centrifuged at $1000 \times g$ for 10 minutes at 4°C. Supernatant fluid (crude cytosolic) was transferred into a new tube. Crude nuclei pellet was washed three times with cold PBS and resuspended by pipetting up and down several times in a buffer that contained 5 mmol/L HEPES, pH 7.9, 1.5 mmol/L MgCl_2 , 0.2 mmol/L EDTA, 0.5 mmol/L dithiothreitol, 26% glycerol (v/v), and 0.325 mol/L NaCl. Nuclei fraction was incubated on ice for 20 minutes. To remove debris, both cytosol and nuclei fractions were centrifuged at $20,000 \times g$ for 20 minutes at 4°C, and supernatant fluids were transferred into a new tube. Protein concentration was determined with the Bradford assay (Bio-Rad).

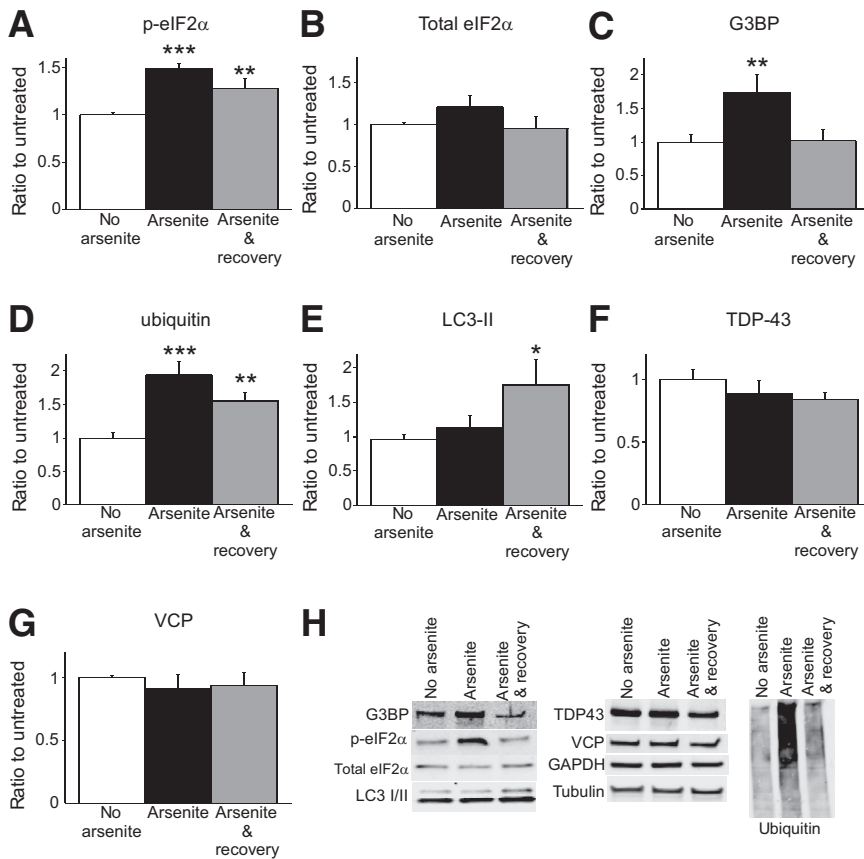


Figure 1 Characterization of arsenite-induced stress granules by immunoblot in C2C12 cells. **A:** Analysis of the cytoplasmic fraction shows an increment in the protein levels of p-eIF2 α immediately after 200 μ mol/L arsenite exposure that diminishes 1 hour after treatment (arsenite and recovery). **B:** Total levels of eIF2 α are unchanged. **C** and **D:** G3BP (**C**) and ubiquitin protein (**D**) levels increase after arsenite treatment in the cytosol. **E:** LC3-II protein levels are up-regulated 1 hour after arsenite treatment. **F** and **G:** Cytoplasmic levels of TDP-43 (**F**) and VCP (**G**) are similar in all conditions. **H:** Representative images of the blots quantified in panels **A–G**. $n = 6$ to 7 (from 4 independent experiments). * $P < 0.05$, ** $P < 0.01$, and *** $P < 0.001$ versus no arsenite. eIF2 α , eukaryotic translation initiation factor 2 α ; G3BP, RasGAP SH3-binding protein; GAPDH, glyceraldehyde-3-phosphate dehydrogenase; LC3, microtubule-associated protein 1A/1B-light chain 3; p, phosphorylated; TDP-43, transactive response DNA-binding protein 43; VCP, valosin-containing protein.

Immunoblotting

Equal amounts of protein were separated onto 4% to 15% Bis-Tris gel and transferred to polyvinylidene difluoride membranes. Membranes were blocked for 1 hour in Odyssey blocking solution (LI-COR Biosciences, Lincoln, NE). After blocking, membranes were incubated 18 to 72 hours with one or two of the following primary antibodies: G3BP (dilution 1:1000; ProteinTech, 13057-2-AP), phosphorylated eIF2 α (S51) (dilution 1:1000; Cell Signaling Technology, Danvers, MA; D9G8), total eIF2 α (dilution 1:1000; Cell Signaling Technology; L57A5), TDP-43 (dilution 1:1000; ProteinTech; 12892-1-AP), ubiquitin (dilution 1:3000; Dako; Z0458), LC3 I/II (dilution 1:3000; Abnova; PAB12534), VCP (dilution 1:5000; Pierce; MA3-004), mono- and polyubiquitylated proteins (dilution 1:1000; Enzo, Farmingdale, NY; FK2), glyceraldehyde-3-phosphate dehydrogenase (dilution 1:5000; Santa Cruz Biotechnology; FL-335), or tubulin (dilution 1:25,000; Sigma-Aldrich; B-5-1-2) in Odyssey blocking solution + 0.2% Tween-20 at 4°C. After washes with TBS + 0.1% Tween-20, membranes were incubated for 1 to 2 hours with the corresponding secondary antibody at a dilution of 1:20,000 (IRDye; LI-COR Biosciences) in TBS + 5% nonfat milk + 0.2% Tween-20 + 0.01% SDS. Blots were scanned in an Odyssey infrared imager (LI-COR Biosciences). Image Studio software version 5.0 (LI-COR Biosciences) was used for blot analysis. Protein levels were normalized to glyceraldehyde-3-phosphate dehydrogenase or tubulin levels.

Statistical Analysis

Comparisons between multiple groups used factorial analysis of variance, followed by Fisher *post hoc* tests. $P \leq 0.05$ was considered significant.

Results

Temporal Resolution of Stress Granules Containing Phosphorylated TDP-43 and Ubiquitin after Acute Arsenite Exposure in C2C12 Cells

C2C12 cells were acutely exposed to the oxidative stress inducer arsenite for 60 minutes at subtoxic concentration of 200 μ mol/L. We then monitored changes in cellular stress responses represented by the formation and resolution of stress granules. Stress granules were identified by staining with TiA-1, an RNA binding protein presented in stress granules.²³ We observed that acute exposure to arsenite significantly triggered the formation of stress granules in most cells (71%). Stress response gradually resolved during the time after arsenite exposure, resulting in only 24% of the cells showing TiA1⁺ stress granules at 60 minutes after arsenite exposure (Supplemental Figure S1A).

We also examined whether TDP-43 and phosphorylated TDP-43 were incorporated and aggregated in these stress granules, because aberrant cytoplasmic inclusions of TDP-43 are commonly observed in skeletal muscle tissue of IBMPFD

and IBM patients.^{7,8} In addition, TDP-43 was shown to play an important role in assembly and maintenance of stress granules.^{24,25} In the acute arsenite exposure, we detected both TDP-43 and phosphorylated TDP-43 (ser409/410) foci that significantly colocalized with TiA-1⁺ stress granules in the cytoplasm of C2C12 cells (Supplemental Figure S1, B–D). TiA-1⁺ stress granules also contained ubiquitin (Supplemental Figure S1, B and E) and, to a lesser extent, LC3 and LAMP2, the autophagosome- and lysosome-associated proteins, respectively (Supplemental Figure S1, B, F–G). However, no colocalization was found between VCP and TDP-43⁺ stress granules after the acute arsenite exposure in C2C12 cells (Supplemental Figure S1H).

Stress granule formation is commonly initiated by phosphorylation of eIF2 α in response to different stressor stimuli. Phosphorylation of eIF2 α inhibits general translation and promotes binding of mRNAs and nucleating RNA binding proteins such as TiA-1.^{26,27} We analyzed cytoplasmic fractions of arsenite-exposed C2C12 cells by immunoblot and found that arsenite induced phosphorylation of eIF2 α , but total eIF2 α cytoplasmic levels remained unchanged (Figure 1, A and B). Increased levels of G3BP, another common component of stress granules, were also observed immediately after arsenite exposure in cytoplasmic fractions (Figure 1C). Consistent with our TiA-1 observations, G3BP returned to basal levels within 1 hour after the exposure (Figure 1C).

On arsenite-exposed cells, we also identified increased cytoplasmic levels of ubiquitin (Figure 1D), together with up-regulation of the specific LC3 isoform recruited in autophagosomes (LC3-II) (Figure 1E). However, we failed to detect changes on cytoplasmic TDP-43 protein levels, suggesting redistribution of available cytoplasmic TDP-43 into stress granules on arsenite exposure (Figure 1F). In addition, cytoplasmic levels of VCP were similar in all conditions (Figure 1G). Representative images of the blots are shown in Figure 1H. Overall, these results indicate that exposure of 200 μ mol/L arsenite for 1 hour reliably induced strong stress granule formation in C2C12 cells. Stress response was resolved for the most part within 60 minutes, including phosphorylation of eIF2 α and formation of stress granules positive for phosphorylated TDP-43 (ser409/410), and ubiquitylated proteins, LC3 and LAMP2. The latter two proteins are members of autophagosomes and lysosomes, respectively, suggesting resolution of arsenite-induced stress granules through autophagy.

To provide evidence that on C2C12 cells stress granules are cleared through autophagy, we incubated cells either for 3 hours with 12 μ mol/L MHY-1485, an mTOR activator that potently inhibits autophagy by suppression of fusion between autophagosomes and lysosomes,²⁸ or for 24 hours with 20 μ mol/L leupeptin, a protease inhibitor that severely impairs lysosomal function. Cells exposed to arsenite and

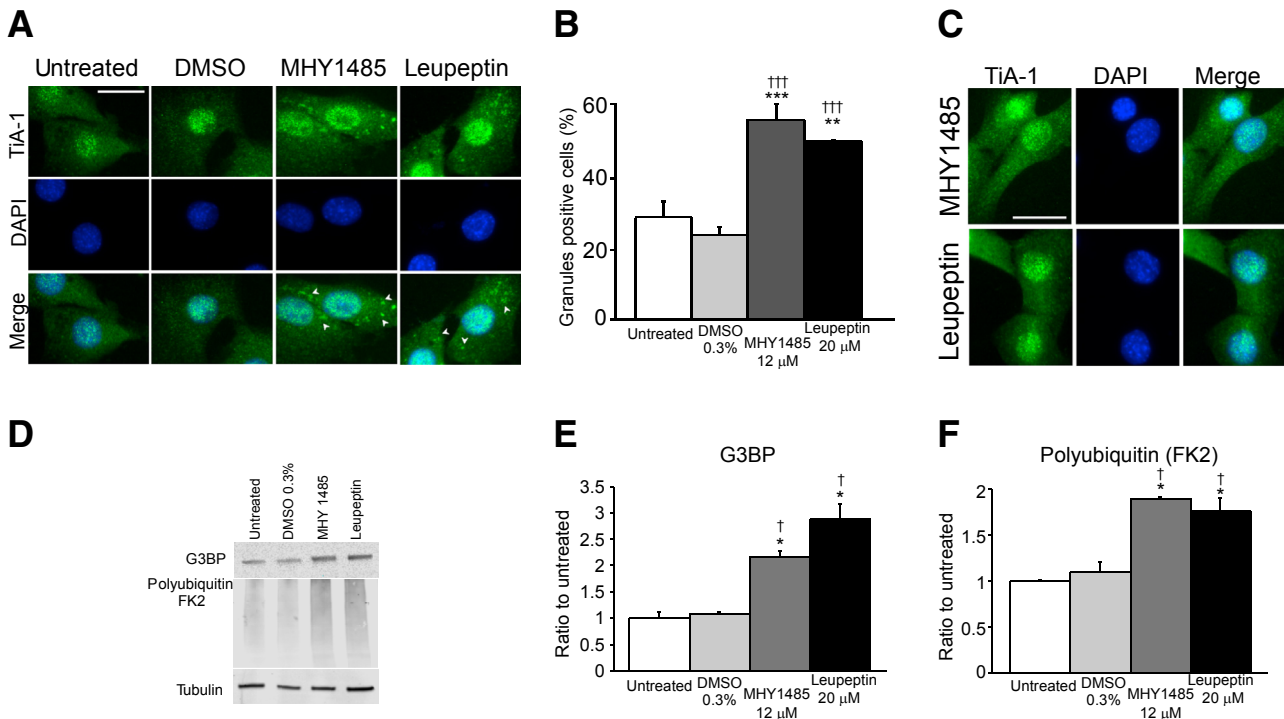


Figure 2 Autophagy and lysosome inhibitors delay stress granule resolution after arsenite exposure. **A:** Cells treated with autophagy (12 μ mol/L MHY1485) or lysosome (20 μ mol/L leupeptin) inhibitors present more stress granules than untreated or 0.3% DMSO-treated cells after left to recover for 1 hour from arsenite exposure. **Arrowheads** indicate stress granules. **B:** Quantification of panel **A**. **C:** MHY1485 and leupeptin treatment does not show stress granules in the absence of arsenite exposure. **D:** Similarly, cells analyzed by immunoblot 1 hour after exposure with 200 μ mol/L arsenite present augmented levels of the stress granule marker G3BP and polyubiquitylated proteins. **E** and **F:** Quantification of panel **D**. $n = 100$ cells per well (3 wells per condition) (**C**). * $P < 0.05$, ** $P < 0.01$, *** $P < 0.001$ versus untreated; † $P < 0.05$, †† $P < 0.001$ versus 0.3% DMSO. Scale bars = 50 μ m (**A** and **C**). DMSO, dimethyl sulfoxide; FK2, mono- and polyubiquitylated proteins antibody; G3BP, RasGAP SH3-binding protein; TiA-1, T-intracellular antigen-1.

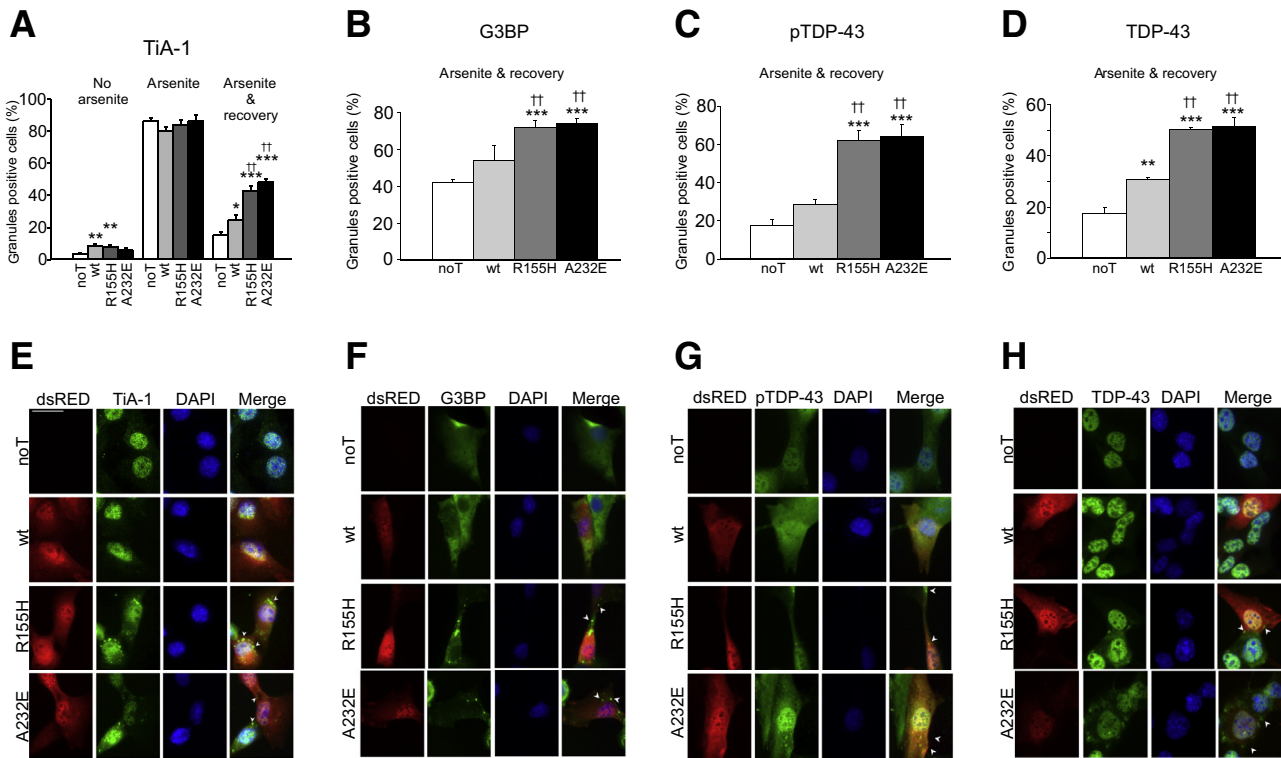


Figure 3 IBMPFD-relevant VCP mutants delay stress granule resolution after arsenite exposure in C2C12 cells. **A:** Cells expressing VCP(R155H) or VCP(A232E) show significantly more TiA-1⁺ stress granules than nontransfected or wt VCP-transfected cells 1 hour after arsenite exposure (right). No differences were observed on untreated cells or immediately after arsenite exposure. **B–D:** Similarly, more G3BP (**B**), pTDP-43⁺ (**C**), and TDP-43⁺ (**D**) granules are observed on cells transfected with mutant VCP than nontransfected and wt-transfected cells, 1 hour after arsenite treatment (arsenite and recovery). **E–H:** Representative images from the arsenite and recovery condition are presented for TiA-1 (**E**), G3BP (**F**), pTDP-43 (**G**), and TDP-43 (**H**). The dsRED tag was fused to the different VCP constructs to allow identification of transfected cells. **Arrowheads** indicate stress granules. *n* = 100 cells per well (6 wells per condition). **P* < 0.05, ***P* < 0.01, and ****P* < 0.001 versus noT. ††*P* < 0.01 versus VCP (wt). Scale bar = 50 μm. G3BP, RasGAP SH3-binding protein; IBMPFD, inclusion body myopathy associated with Paget disease of bone and frontotemporal dementia; noT, nontransfected; p, phosphorylated; TDP-43, transactive response DNA-binding protein 43; TiA-1, T-intracellular antigen-1; VCP, valosin-containing protein; wt, wild-type.

allowed to recover for 1 hour presented a significant larger number of cytoplasmic TiA-1⁺ stress granules when treated with MHY-1485 or leupeptin period (**Figure 2, A and B**) compared with untreated and dimethyl sulfoxide groups (untreated = 28%; dimethyl sulfoxide = 23%; MHY1485 = 55%; leupeptin = 49%); supporting the fact that the autophagy/lysosome pathway plays an important role in stress granule resolution on C2C12 cells. Consistently, immunoblot analysis found G3BP and polyubiquitylated protein level increments on the MHY-1485- and leupeptin-treated lysates of cells allowed to recuperate for 60 minutes after arsenite treatment (**Figure 2, D–F**). Importantly, MHY-1485 or leupeptin incubation without arsenite treatment did not induce a stress response, and no stress granules were detected (**Figure 2C**).

IBMPFD-Relevant VCP Mutants Impair the Resolution of Arsenite-Induced Stress Granules in Undifferentiated and Differentiated C2C12 Cells

To determine whether mutations in VCP significantly affect cellular stress response, we transiently transfected C2C12

cells with one of the following constructs: human VCP(wt), VCP(R155H), or VCP(A232E) fused to dsRED and monitored the formation and resolution of stress granules after acute arsenite exposure. We found a small, but significant increase of stress granule-positive cells because of transfection on cells with no arsenite exposure [no transfected (noT) = 3%; VCP(wt) = 8%; VCP(R155H) = 8%; VCP(A232E) = 6%] (**Figure 3A**). However, no significant effects were observed among the different transfection conditions immediately after the 60 minutes of arsenite incubation (**Figure 3A**). Importantly, we found that mutant VCP-transfected cells failed to resolve significant numbers of stress granules even 60 minutes after exposure [noT = 15%; VCP(wt) = 24%; VCP(R155H) = 43%; VCP(A232E) = 48%] (**Figure 3, A and E**), indicating that VCP is involved in the clearance of stress granules, and that mutations on VCP impair this process, causing an abnormally prolonged cellular stress response. Similarly, significant number of cytoplasmic stress granules positive for G3BP (**Figure 3, B and F**), phosphorylated TDP-43 (ser409/410) (**Figure 3, C and G**), and total TDP-43 (**Figure 3, D and H**) were observed on cells transfected

with mutant VCP compared with noT and VCP(wt) groups that had a 60-minute recovery period after arsenite exposure.

In addition, impaired stress granule resolution was observed on differentiated C2C12 cells transfected with mutant VCP. Cells incubated on horse serum for 5 days expressed myosin and showed dsRED⁺ expression when transfected (Figure 4A). Differentiated C2C12 cells that express mutant VCP presented significantly more TiA-1⁺ stress granules than noT and VCP(wt) expressing cells when incubated with arsenite and allowed to recover for 60 minutes [noT = 17%; VCP(wt) = 33%; VCP(R155H) = 78%; VCP(A232E) = 79%] (Figure 4, B and C). All together, these findings indicate that mutant VCP impaired oxidative stress response by hindering stress granule resolution.

IBMPFD-Relevant VCP Mutants Do Not Impair the Resolution of Heat Shock–Induced Cellular Stress Response in C2C12 Cells

We next examined whether mutant VCP also impaired the resolution of stress granules with the use of a different type of exogenous cellular stress. Heat shock is one of the best characterized cellular stressors and produces stress granules in a wide variety of cells.²³ We, therefore, incubated C2C12 cells at 42°C for 30 minutes to induce heat shock, and we observed cytoplasmic stress granules in 99% of the cells. The number of cytoplasmic TiA-1⁺ puncta decreased by 51% at 30 minutes of recovery, by 70% at 1 hour of recovery, and by 75% at 2 hours of recovery (Supplemental Figure S2A). Similar to arsenite-induced granules, heat shock–induced stress granules were positive for TDP-43 (Supplemental Figure S2, B and C), phosphorylated TDP-43 (ser409/410) (Supplemental Figure S2, B and D), ubiquitin (Supplemental Figure S2, B and E), and the autophagosome- and lysosome-associated proteins, LC3 and LAMP2 (Supplemental Figure S2, B, F–H) but negative for VCP (Supplemental Figure S2H).

We then transfected C2C12 cells with human VCP(wt), VCP(R155H), or VCP(A232E) fused to dsRED and quantitatively examined cytoplasmic stress granules on untreated cells, cells incubated for 30 minutes at 42°C, and cells that recovered for 30 minutes after 42°C incubation (Figure 5A). We did not find significant effects among the different transfection conditions on untreated cells or immediately after 42°C incubation (Figure 5A). Surprisingly, we did not observe any significant delay either in resolving the heat shock–induced cellular stress responses between wt and mutant VCP-transfected C2C12 cells (Figure 5, A and B). The number of cytoplasmic TiA-1⁺ puncta was 33% for wt, 35% for R155H, and 32% for A232E at 30 minutes of recovery (Figure 5A). These findings suggest that stress granules produced by different kinds of stressors are not resolved by exactly the same mechanisms and that, at least on C2C12 cells, VCP may be dispensable for the clearance of stress granules produced by some cellular insults.

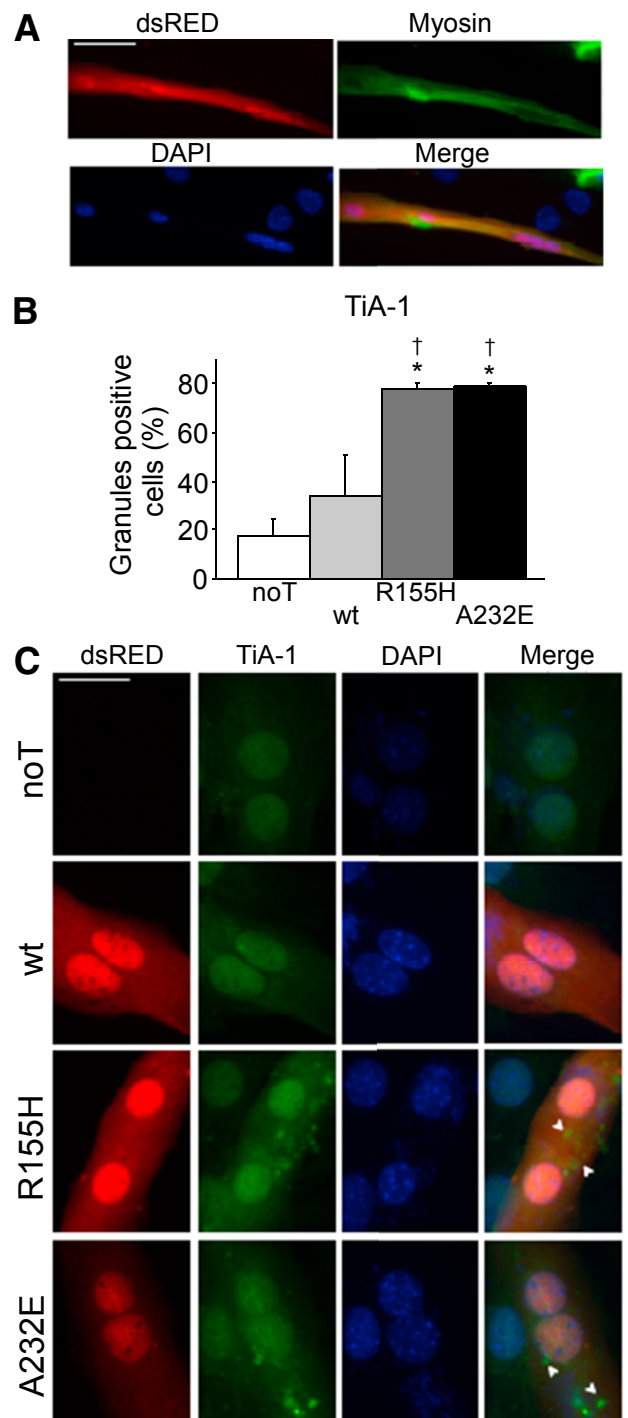


Figure 4 IBMPFD-relevant VCP mutants delay stress granule resolution in differentiated C2C12 cells. **A:** Cells express myosin protein after 5 days of incubation in horse serum 2% and show dsRED⁺ expression when transfected. **B:** Differentiated C2C12 cells that expressed VCP(R155H) or VCP(A232E) show significantly more TiA-1⁺ stress granules than nontransfected or wt VCP-transfected cells when left to recover for 1 hour after arsenite exposure. **C:** Representative images from the data graphed on panel B. The dsRED tag was fused to the different VCP constructs to allow identification of transfected cells. **Arrowheads** indicate stress granules. *n* = 50 cells per well (6 wells per condition). **P* < 0.05 versus noT; †*P* < 0.05 versus wt VCP. Scale bars: 50 μm (A); 25 μm (C). IBMPFD, inclusion body myopathy associated with Paget disease of bone and frontotemporal dementia; noT, nontransfected; TiA-1, T-intracellular antigen-1; VCP, valosin-containing protein; wt, wild-type.

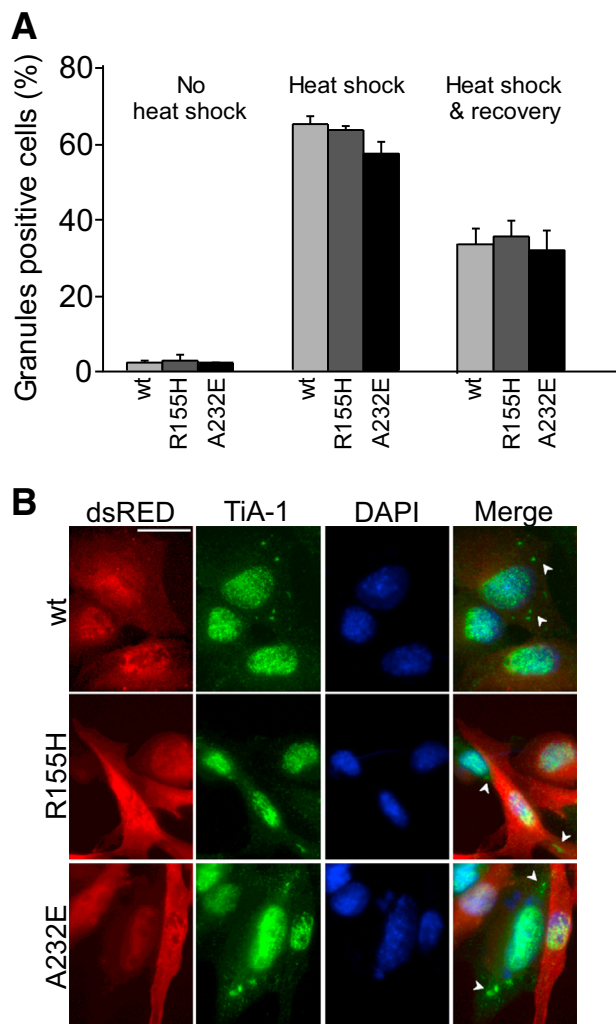


Figure 5 IBMPFD-relevant VCP mutants do not delay stress granule resolution after heat shock treatment in C2C12 cells. **A:** Cells expressing VCP(R155H) or VCP(A232E) show similar TiA-1⁺ stress granules compared with wt VCP-expressing cells on all conditions: no treatment, immediately after heat shock, or 30 minutes after heat shock (right). **B:** Representative images of the heat shock and recovery condition. The dsRED tag was fused to the different VCP constructs to allow identification of transfected cells. **Arrowheads** indicate stress granules. $n = 100$ cells per well (7 to 8 wells per condition). Scale bar = 50 μm . IBMPFD, inclusion body myopathy associated with Paget disease of bone and frontotemporal dementia; TiA-1, T-intracellular antigen-1; VCP, valosin-containing protein; wt, wild-type.

The VCP_{R155H}-KI Mouse Model Shows Elevated Oxidative Stress but Not Increments on the Steady-State Levels of Stress Granule Markers

In 2010, Kimonis and colleagues²⁹ generated a KI mouse model of IBMPFD, which expresses a disease-relevant VCP mutation (R155H) in physiologically relevant levels. This model presents muscle, bone, and brain pathologic characteristics similar to VCP-associated disease in patients.⁵ For muscle pathology, the VCP_{R155H}-KI mouse develops significant progressive muscle weakness and shows increased cytoplasmic ubiquitin deposits and autophagy

dysregulation.³⁰ Autophagy is a process that helps to deal with cellular stress and plays an important role in quality control functions.²⁹ Therefore, with the use of the VCP_{R155H}-KI mouse as a model, we explored whether mutant VCP leads to elevated levels of cellular stress and alterations on the stress granule pathway. Consistent with previous reports,²⁹ we observed that aged (15- to 18-month-old) heterozygous VCP_{R155H}-KI mice showed significant increments of ubiquitinated proteins on skeletal muscle compared with age-matched wt littermates (Figure 6A). We also analyzed the basal levels of oxidated proteins and found that skeletal muscle of VCP_{R155H}-KI mice present increased amounts compared with wt muscle samples (Figure 6B). These findings indicate that skeletal muscle from VCP_{R155H}-KI mice exhibit chronic cellular and oxidative stress. We then addressed whether steady-state levels of the stress granule pathway were altered in the VCP_{R155H}-KI mouse. Despite showing increased oxidative stress, we did not observe differences on the levels of the stress granule markers G3BP, phosphorylated eIF2 α , or poly(A)-binding protein 1 on VCP_{R155H}-KI mice muscle (Figure 6, C–G). Furthermore, hematoxylin and eosin staining revealed no major histologic differences between genotypes (Figure 6I). Finally, TDP-43 and the stress granule markers G3BP and TiA-1 showed similar staining on wt and VCP_{R155H}-KI skeletal muscle by immunofluorescence (Figure 6, J–L). Specifically, TiA-1⁺ and TDP-43⁺ signal was predominantly detected together with DAPI, indicating major nuclear localization of these two proteins (Figure 6H). Together, these results suggest that cumulative oxidative stress produced by aging may not be a sufficient condition to trigger the delayed resolution of the stress granule response, but additional cellular stress, possibly from exogenous origin (eg, arsenite exposure), may be required to exhibit pathologic dysregulation of the stress granule pathway caused by mutant VCP on muscle tissue.

Discussion

One of the physiologic functions of VCP is to alleviate cellular stress.¹⁰ In this study, we transiently transfected myoblast C2C12 cells with mutant VCP and observed slower clearance of TiA-1⁺ stress granules after arsenite exposure. Similarly, immunofluorescence staining for G3BP, total TDP-43, and phosphorylated TDP-43 showed delayed resolution of stress granules on oxidative stress. Our findings indicate that IBMPFD-relevant VCP mutations impair the resolution of acutely induced oxidative cellular stress. This is important because skeletal muscle cells are frequently exposed to diverse endogenous or exogenous kinds of stress and require effective mechanisms to cope with these insults. Attenuated tolerance to oxidative stress may, therefore, result in muscle degeneration.

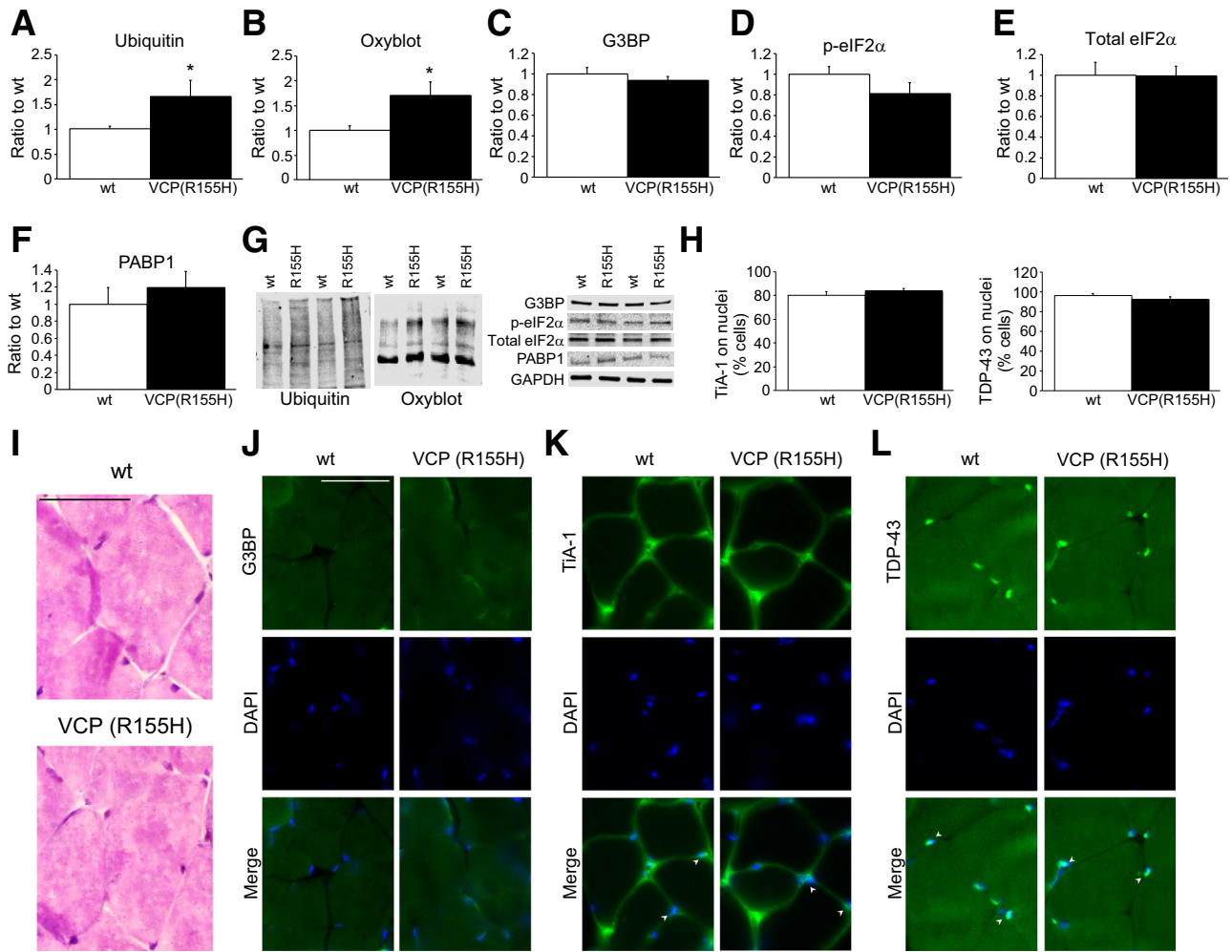


Figure 6 Oxidative stress but not stress granule markers are increased in the IBMPFD model: the VCP_{R155H}-KI mouse. **A:** Immunoblot analysis of skeletal muscle lysates shows augmented ubiquitylated proteins on 15- to 18-month-old VCP_{R155H}-KI mice compared with wt skeletal muscle lysates of the same age. **B:** Similarly, the oxyblot assay reveals increments on oxidated proteins on skeletal muscle of VCP_{R155H}-KI mice compared with wt mice. **C–F:** However, G3BP (**C**), p-eIF2 α (**D**), total eIF2 α (**E**), and PABP1 (**F**) protein levels are similar between genotypes. **G:** Representative blots for the different proteins analyzed. **H:** TiA-1 and TDP-43 present major nuclear localization when analyzed by immunofluorescence. **I:** Hematoxylin and eosin staining shows no major histologic differences between the wt and VCP_{R155H}-KI skeletal muscle. **J–L:** Similarly, no differences are detected when skeletal muscle was stained for G3BP (**J**), TiA-1 (**K**), and TDP-43 (**L**). **Arrowheads** indicate nuclear localization of TiA-1 and TDP-43 proteins. $n = 8$ wt and 7 VCP_{R155H}-KI (R155H) mice (**G**). * $P < 0.05$. Scale bars = 50 μ m. eIF2 α , eukaryotic translation initiation factor 2 α ; GAPDH, glyceraldehyde-3-phosphate dehydrogenase; G3BP, RasGAP SH3-binding protein; IBMPFD, inclusion body myopathy associated with Paget disease of bone and frontotemporal dementia; KI, knockin; p, phosphorylated; PABP1, poly(A)-binding protein 1; TDP-43, transactive response DNA-binding protein 43; TiA-1, T-intracellular antigen-1; VCP, valosin-containing protein; wt, wild-type.

The connection between stress granules and degenerative diseases that present protein aggregates has become increasingly clear.²⁷ TDP-43 is an example of a RNA binding protein, whose mutations lead to cytoplasmic protein inclusions and neurodegeneration. Pathologic TDP-43 accumulates as insoluble aggregates in neurons and/or glia of patients with frontotemporal lobar degeneration, ALS, and IBMPFD.^{9,29,31–33} TDP-43 aggregates are also developed in the cytosol of skeletal muscle fibers in IBM and IBMPFD.^{7,8} However, under physiologic conditions, TDP-43, like other RNA binding proteins, aggregates in the reversible and highly regulated process that gives rise to stress granules.^{25,34,35} Specifically, it is involved in maturation of stress

granules that contain G3BP, and was shown to colocalize with stress granules that contain TiA-1 or ubiquitin.^{24,25,35–37} In animal models, ALS-relevant TDP-43 mutations were reported to produce larger stress granules than wt TDP-43,^{37,38} consistent with an altered stress response. Here, we observed that cellular stress produces TDP-43 recruitment to stress granules in C2C12 cells. Mutant VCP keeps TDP-43 within stress granules for abnormal periods of time, and this could favor pathologic TDP-43 aggregation. Consistently, it has been shown that TDP-43 accumulation in stress granules can progress to stable cytosolic aggregates.³⁹

Pathologic TDP-43 inclusions are ubiquitylated and phosphorylated.³¹ In particular, phosphorylation of S409/

410 of TDP-43 is commonly observed in frontotemporal lobar degeneration and ALS, among other neurodegenerative diseases.⁴⁰ Phosphorylated TDP43 was shown to be more resistant to degradation by the ubiquitin-proteasome system than its not phosphorylated counterpart,⁴¹ and TDP43 phosphorylation is tightly correlated with its aggregation.⁴² Therefore, it has been suggested that phosphorylation is an early pathologic event that contributes to TDP-43 buildup.⁴² However, we observed this particular site of TDP-43 to be phosphorylated and recruited to stress granules on cellular stress, indicating that S409/410 phosphorylation has a relevant functional role in stress granule dynamics.

Intracellular protein degradation happens mainly through the ubiquitin-proteasome system and the autophagosome/lysosome pathway. In both these cellular processes, VCP plays a central role by binding either directly or through partners to ubiquitylated proteins to sort them to one of these cellular compartments.^{11,43} Accordingly, IBMPFD-relevant VCP mutations alter both these pathways.⁴⁴ Particularly, mutant VCP isoforms were reported to dysregulate proteasome activity and induce apoptosis.^{45,46} In addition, it was shown that mutant VCP produces disruption of autophagosome-lysosome fusion in muscle tissue.⁶ Moreover, primary myoblasts of IBMPFD patients revealed accumulation of LC3-II, suggesting dysregulation of autophagy.^{29,47} Similarly, increased protein levels of LC3-II and p62 were reported in transgenic mice that expressed VCP(R155H).^{29,44}

Stress granule formation is a highly regulated process that starts with translocation of nucleating RNA binding proteins from the nucleus to the cytoplasm where they encounter and bind mRNAs.¹³ Stress granules are initially small but rapidly recruit many more mRNAs and RNA binding proteins to generate mature stress granules. RNA binding proteins not only interact with RNA but with each other through glycine-rich domains and are therefore susceptible to aggregation.²⁶ Stress response is resolved by dissolution of stress granules and reinitiation of RNA translation once stress is removed.^{23,26,27} Here, we observed that mutant VCP delays stress granule resolution. This finding is consistent with reports that suggest VCP participation in clearance of stress granules.^{14,15} Recently, it was reported that autophagy or lysosome or VCP inhibition produces impairments on either stress granule resolution or composition.^{14,15} These observations led to the proposal that autophagy underlies VCP-mediated stress granule clearance,^{14,15} and that this process may depend on ubiquitin tagging. Consistent with this idea, stress granules are heavily ubiquitylated complexes,⁴⁸ and inhibition of ubiquitin-proteasome system induces stress granule formation.⁴⁹ Consistently, Tresse et al.¹² reported that VCP is essential for autophagy-mediated degradation of ubiquitylated substrates and that this function is disrupted on IBMPFD-relevant VCP mutations.

Although several key processes altered by IBMPFD-relevant mutations were identified, the exact pathogenic

mechanisms that lead to disease remain unclear. Our results strengthen the hypothesis that mutations on VCP generate dysregulation of the stress response by diminishing resolution of stress granules. Impaired ability to recovery from cellular stress may result in chronic overactive response and skeletal muscle degeneration.

Acknowledgment

Human VCP(wt), VCP(R155H), or VCP(A232E) fused to dsRED constructs were kindly provided by Dr. J. Paul Taylor (St. Jude Children's Research Hospital, Memphis, TN).

Supplemental Data

Supplemental material for this article can be found at <http://dx.doi.org/10.1016/j.ajpath.2016.02.007>.

References

1. Kimonis VE, Kovach MJ, Waggoner B, Leal S, Salam A, Rimer L, Davis K, Khardori R, Gelber D: Clinical and molecular studies in a unique family with autosomal dominant limb-girdle muscular dystrophy and Paget disease of bone. *Genet Med* 2000, 2:232–241
2. Watts GD, Wymer J, Kovach MJ, Mehta SG, Mumm S, Darvish D, Pestronk A, Whyte MP, Kimonis VE: Inclusion body myopathy associated with Paget disease of bone and frontotemporal dementia is caused by mutant valosin-containing protein. *Nat Genet* 2004, 36:377–381
3. Johnson JO, Mandrioli J, Benatar M, Abramzon Y, Van Deerlin VM, Trojanowski JQ, et al: Exome sequencing reveals VCP mutations as a cause of familial ALS. *Neuron* 2010, 68:857–864
4. Kimonis VE, Fulchiero E, Vesa J, Watts G: VCP disease associated with myopathy, Paget disease of bone and frontotemporal dementia: review of a unique disorder. *Biochim Biophys Acta* 2008, 1782:744–748
5. Nalbandian A, Donkervoort S, Dec E, Badadani M, Katheria V, Rana P, Nguyen C, Mukherjee J, Caiozzo V, Martin B, Watts GD, Vesa J, Smith C, Kimonis VE: The multiple faces of valosin-containing protein-associated diseases: inclusion body myopathy with Paget's disease of bone, frontotemporal dementia, and amyotrophic lateral sclerosis. *J Mol Neurosci* 2011, 45:522–531
6. Ju JS, Fuentealba RA, Miller SE, Jackson E, Piwnicka-Worms D, Baloh RH, Weihl CC: Valosin-containing protein (VCP) is required for autophagy and is disrupted in VCP disease. *J Cell Biol* 2009, 187:875–888
7. Weihl CC, Temiz P, Miller SE, Watts G, Smith C, Forman M, Hanson PI, Kimonis V, Pestronk A: TDP-43 accumulation in inclusion body myopathy muscle suggests a common pathogenic mechanism with frontotemporal dementia. *J Neurol Neurosurg Psychiatry* 2008, 79:1186–1189
8. Salajegheh M, Pinkus JL, Taylor JP, Amato AA, Nazareno R, Baloh RH, Greenberg SA: Sarcoplasmic redistribution of nuclear TDP-43 in inclusion body myositis. *Muscle Nerve* 2009, 40:19–31
9. Custer SK, Neumann M, Lu H, Wright AC, Taylor JP: Transgenic mice expressing mutant forms VCP/p97 recapitulate the full spectrum of IBMPFD including degeneration in muscle, brain and bone. *Hum Mol Genet* 2010, 19:1741–1755

10. Dargemont C, Ossareh-Nazari B: Cdc48/p97, a key actor in the interplay between autophagy and ubiquitin/proteasome catabolic pathways. *Biochim Biophys Acta* 2011, 1823:138–144
11. Richly H, Rape M, Braun S, Rumpf S, Hoegge C, Jentsch S: A series of ubiquitin binding factors connects CDC48/p97 to substrate multiubiquitylation and proteasomal targeting. *Cell* 2005, 120: 73–84
12. Tresse E, Salomons FA, Vesa J, Bott LC, Kimonis V, Yao TP, Dantuma NP, Taylor JP: VCP/p97 is essential for maturation of ubiquitin-containing autophagosomes and this function is impaired by mutations that cause IBMPFD. *Autophagy* 2010, 6:217–227
13. Kedersha N, Cho MR, Li W, Yacono PW, Chen S, Gilks N, Golan DE, Anderson P: Dynamic shuttling of TIA-1 accompanies the recruitment of mRNA to mammalian stress granules. *J Cell Biol* 2000, 151: 1257–1268
14. Buchan JR, Kolaitis RM, Taylor JP, Parker R: Eukaryotic stress granules are cleared by autophagy and Cdc48/VCP function. *Cell* 2013, 153:1461–1474
15. Seguin SJ, Morelli FF, Vinet J, Amore D, De Biasi S, Poletti A, Rubinsztein DC, Carra S: Inhibition of autophagy, lysosome and VCP function impairs stress granule assembly. *Cell Death Differ* 2014, 21: 1838–1851
16. Vinceti M, Bottecchi I, Fan A, Finkelstein Y, Mandrioli J: Are environmental exposures to selenium, heavy metals, and pesticides risk factors for amyotrophic lateral sclerosis? *Rev Environ Health* 2012, 27: 19–41
17. Lindsay J, Laurin D, Verreault R, Hebert R, Helliwell B, Hill GB, McDowell I: Risk factors for Alzheimer's disease: a prospective analysis from the Canadian Study of Health and Aging. *Am J Epidemiol* 2002, 156:445–453
18. Lim KT, Shukor MY, Wasoh H: Physical, chemical, and biological methods for the removal of arsenic compounds. *Biomed Res Int* 2014, 2014:503784
19. Watanabe T, Hirano S: Metabolism of arsenic and its toxicological relevance. *Arch Toxicol* 2013, 87:969–979
20. Liu J, Kadiiska MB, Liu Y, Lu T, Qu W, Waalkes MP: Stress-related gene expression in mice treated with inorganic arsenicals. *Toxicol Sci* 2001, 61:314–320
21. Bernstam L, Nriagu J: Molecular aspects of arsenic stress. *J Toxicol Environ Health B Crit Rev* 2000, 3:293–322
22. Committee for the Update of the Guide for the Care and Use of Laboratory Animals; National Research Council: *Guide for the Care and Use of Laboratory Animals: Eighth Edition*. Washington, DC, National Academies Press, 2011
23. Thomas MG, Loschi M, Desbats MA, Boccaccio GL: RNA granules: the good, the bad and the ugly. *Cell Signal* 2010, 23:324–334
24. Fiesel FC, Voigt A, Weber SS, Van den Haute C, Waldenmaier A, Gorner K, Walter M, Anderson ML, Kern JV, Rasse TM, Schmidt T, Springer W, Kirchner R, Bonin M, Neumann M, Baekelandt V, Alunni-Fabbroni M, Schulz JB, Kahle PJ: Knockdown of transactive response DNA-binding protein (TDP-43) downregulates histone deacetylase 6. *EMBO J* 2010, 29:209–221
25. McDonald KK, Aulas A, Destroismaisons L, Pickles S, Beleac E, Camu W, Rouleau GA, Vande Velde C: TAR DNA-binding protein 43 (TDP-43) regulates stress granule dynamics via differential regulation of G3BP and TIA-1. *Hum Mol Genet* 2011, 20: 1400–1410
26. Kedersha NL, Gupta M, Li W, Miller I, Anderson P: RNA-binding proteins TIA-1 and TIAR link the phosphorylation of eIF-2 alpha to the assembly of mammalian stress granules. *J Cell Biol* 1999, 147: 1431–1442
27. Wolozin B: Regulated protein aggregation: stress granules and neurodegeneration. *Mol Neurodegener* 2012, 7:56
28. Choi YJ, Park YJ, Park JY, Jeong HO, Kim DH, Ha YM, Kim JM, Song YM, Heo HS, Yu BP, Chun P, Moon HR, Chung HY: Inhibitory effect of mTOR activator MHY1485 on autophagy: suppression of lysosomal fusion. *PLoS One* 2012, 7:e43418
29. Badadani M, Nalbandian A, Watts GD, Vesa J, Kitazawa M, Su H, Tanaja J, Dec E, Wallace DC, Mukherjee J, Caiozzo V, Warman M, Kimonis VE: VCP associated inclusion body myopathy and paget disease of bone knock-in mouse model exhibits tissue pathology typical of human disease. *PLoS One* 2010, 5: e13183
30. Nalbandian A, Llewellyn KJ, Badadani M, Yin HZ, Nguyen C, Katheria V, Watts G, Mukherjee J, Vesa J, Caiozzo V, Mozaffar T, Weiss JH, Kimonis VE: A progressive translational mouse model of human valosin-containing protein disease: the VCP(R155H/+) mouse. *Muscle Nerve* 2013, 47:260–270
31. Neumann M, Sampathu DM, Kwong LK, Truax AC, Micsenyi MC, Chou TT, Bruce J, Schuck T, Grossman M, Clark CM, McCluskey LF, Miller BL, Masliah E, Mackenzie IR, Feldman H, Feiden W, Kretzschmar HA, Trojanowski JQ, Lee VM: Ubiquitinated TDP-43 in frontotemporal lobar degeneration and amyotrophic lateral sclerosis. *Science* 2006, 314:130–133
32. Sreedharan J, Blair IP, Tripathi VB, Hu X, Vance C, Rogelj B, Ackerley S, Durnall JC, Williams KL, Buratti E, Baralle F, de Belleruche J, Mitchell JD, Leigh PN, Al-Chalabi A, Miller CC, Nicholson G, Shaw CE: TDP-43 mutations in familial and sporadic amyotrophic lateral sclerosis. *Science* 2008, 319: 1668–1672
33. Kabashi E, Valdmanis PN, Dion P, Spiegelman D, McConkey BJ, Vande Velde C, Bouchard JP, Lacomblez L, Pochigavaeva K, Salachas F, Pradat PF, Camu W, Meininger V, Dupre N, Rouleau GA: TARDBP mutations in individuals with sporadic and familial amyotrophic lateral sclerosis. *Nat Genet* 2008, 40:572–574
34. Wang IF, Wu LS, Chang HY, Shen CK: TDP-43, the signature protein of FTL-D-U, is a neuronal activity-responsive factor. *J Neurochem* 2008, 105:797–806
35. Colombrita C, Zennaro E, Fallini C, Weber M, Sommacal A, Buratti E, Silani V, Ratti A: TDP-43 is recruited to stress granules in conditions of oxidative insult. *J Neurochem* 2009, 111: 1051–1061
36. Cairns NJ, Neumann M, Bigio EH, Holm IE, Troost D, Hatanpaa KJ, Foong C, White CL 3rd, Schneider JA, Kretzschmar HA, Carter D, Taylor-Reinwald L, Paulsmeier K, Strider J, Gitcho M, Goate AM, Morris JC, Mishra M, Kwong LK, Stieber A, Xu Y, Forman MS, Trojanowski JQ, Lee VM, Mackenzie IR: TDP-43 in familial and sporadic frontotemporal lobar degeneration with ubiquitin inclusions. *Am J Pathol* 2007, 171:227–240
37. Liu-Yesucevitz L, Bilgutay A, Zhang YJ, Vanderweyde T, Citro A, Mehta T, Zaarur N, McKee A, Bowser R, Sherman M, Petrucelli L, Wolozin B: Tar DNA binding protein-43 (TDP-43) associates with stress granules: analysis of cultured cells and pathological brain tissue. *PLoS One* 2010, 5:e13250
38. Dewey CM, Cenik B, Sephton CF, Dries DR, Mayer P 3rd, Good SK, Johnson BA, Herz J, Yu G: TDP-43 is directed to stress granules by sorbitol, a novel physiological osmotic and oxidative stressor. *Mol Cell Biol* 2011, 31:1098–1108
39. Parker SJ, Meyerowitz J, James JL, Liddell JR, Crouch PJ, Kanninen KM, White AR: Endogenous TDP-43 localized to stress granules can subsequently form protein aggregates. *Neurochem Int* 2012, 60:415–424
40. Neumann M, Kwong LK, Lee EB, Kremmer E, Flatley A, Xu Y, Forman MS, Troost D, Kretzschmar HA, Trojanowski JQ, Lee VM: Phosphorylation of S409/410 of TDP-43 is a consistent feature in all sporadic and familial forms of TDP-43 proteinopathies. *Acta Neuropathol* 2009, 117:137–149
41. Zhang YJ, Gendron TF, Xu YF, Ko LW, Yen SH, Petrucelli L: Phosphorylation regulates proteasomal-mediated degradation and solubility of TAR DNA binding protein-43 C-terminal fragments. *Mol Neurodegener* 2010, 5:33
42. Lee EB, Lee VM, Trojanowski JQ: Gains or losses: molecular mechanisms of TDP43-mediated neurodegeneration. *Nat Rev Neurosci* 2011, 13:38–50

43. Jentsch S, Rumpf S: Cdc48 (p97): a “molecular gearbox” in the ubiquitin pathway? *Trends Biochem Sci* 2007, 32:6–11
44. Ju JS, Weihl CC: p97/VCP at the intersection of the autophagy and the ubiquitin proteasome system. *Autophagy* 2010, 6: 283–285
45. Forman MS, Mackenzie IR, Cairns NJ, Swanson E, Boyer PJ, Drachman DA, Jhaveri BS, Karlawish JH, Pestronk A, Smith TW, Tu PH, Watts GD, Markesbery WR, Smith CD, Kimonis VE: Novel ubiquitin neuropathology in frontotemporal dementia with valosin-containing protein gene mutations. *J Neuropathol Exp Neurol* 2006, 65:571–581
46. Gitcho MA, Strider J, Carter D, Taylor-Reinwald L, Forman MS, Goate AM, Cairns NJ: VCP mutations causing frontotemporal lobar degeneration disrupt localization of TDP-43 and induce cell death. *J Biol Chem* 2009, 284:12384–12398
47. Vesa J, Su H, Watts GD, Krause S, Walter MC, Martin B, Smith C, Wallace DC, Kimonis VE: Valosin containing protein associated inclusion body myopathy: abnormal vacuolization, autophagy and cell fusion in myoblasts. *Neuromuscul Disord* 2009, 19:766–772
48. Kwon S, Zhang Y, Matthias P: The deacetylase HDAC6 is a novel critical component of stress granules involved in the stress response. *Genes Dev* 2007, 21:3381–3394
49. Mazroui R, Di Marco S, Kaufman RJ, Gallouzi IE: Inhibition of the ubiquitin-proteasome system induces stress granule formation. *Mol Biol Cell* 2007, 18:2603–2618